

## Supplementary Information (SI)

### Cyclic ether-based electrolyte solutions for potassium metal batteries

Roy Heyns <sup>a</sup>, Robert Markowski <sup>b</sup>, Andrii Kachmar <sup>b</sup>, Johannes Ingenmey <sup>c</sup>, Wouter Monnens <sup>d</sup>, Alexandru Vlad <sup>b,e</sup>, Barbara Kirchner <sup>c</sup>, Jan Fransaer <sup>d</sup> and Koen Binnemans <sup>a\*</sup>

<sup>a</sup> KU Leuven, Department of Chemistry, Celestijnenlaan 200F, P.O. box 2404, B-3001 Leuven, Belgium.

<sup>b</sup> UC Louvain, Institute of Condensed Matter and Nanosciences, Place L. Pasteur 1, B-1348 Louvain-la-Neuve, Belgium

<sup>c</sup> University of Bonn, Mulliken Center for Theoretical Chemistry, Bonn D-53115, Germany

<sup>d</sup> KU Leuven, Department of Materials Engineering, Kasteelpark Arenberg 44, B-3001 Leuven, Belgium.

<sup>e</sup> WEL Research Institute, avenue Pasteur, 6, 1300 Wavre, Belgium

\*Corresponding author:

Email: [Koen.Binnemans@kuleuven.be](mailto:Koen.Binnemans@kuleuven.be)

**Table S1.** Ionic conductivity ( $\kappa$ ), dynamic viscosity ( $\eta$ ), density ( $\rho$ ), and  $K^+$  concentration ( $c_{K^+}$ ) of THF-KFSI electrolyte solutions, measured at 25 °C.

Solvent-to-salt mole ratio	$\kappa$ at 25 °C (mS cm <sup>-1</sup> )	$\eta$ at 25 °C (mPa×s)	$\rho$ at 25 °C (g cm <sup>-3</sup> )	$c_{K^+}$ (mol L <sup>-1</sup> )
50:1	2.4	0.6	0.92	0.24
40:1	2.7	0.6	0.93	0.30
30:1	4.2	0.7	0.94	0.39
20:1	5.8	0.8	0.97	0.58
15:1	7.3	0.9	0.99	0.76
12:1	8.2	1.2	1.02	0.94
10:1	9.4	1.3	1.04	1.11
9:1	9.7	1.5	1.06	1.22
8:1	10.4	1.8	1.07	1.35
7:1	11.7	2.1	1.10	1.51
6:1	12.7	2.5	1.12	1.72
5:1	12.6	3.5	1.16	2.00
4:1	11.5	5.1	1.21	2.38
3:1	11.1	9.3	1.28	2.94

**Table S2.** Ionic conductivity ( $\kappa$ ), dynamic viscosity ( $\eta$ ), density ( $\rho$ ), and  $K^+$  concentration ( $c_{K^+}$ ) of MeTHF-KFSI electrolyte solutions, measured at 25 °C.

Solvent-to-salt mole ratio	$\kappa$ at 25 °C (mS cm <sup>-1</sup> )	$\eta$ at 25 °C (mPa×s)	$\rho$ at 25 °C (g cm <sup>-3</sup> )	$c_{K^+}$ (mol L <sup>-1</sup> )
50:1	0.3	0.5	0.88	0.19
40:1	0.4	0.6	0.88	0.24
30:1	0.7	0.7	0.90	0.32
20:1	1.3	0.8	0.92	0.47
15:1	1.9	0.8	0.94	0.62
12:1	2.6	1.0	0.96	0.77
10:1	3.5	1.2	0.98	0.91
9:1	3.5	1.4	1.00	1.00
8:1	3.9	1.5	1.01	1.11
7:1	4.7	1.9	1.03	1.26
6:1	5.4	2.2	1.06	1.44
5:1	5.7	3.1	1.09	1.68
4:1	6.4	4.8	1.14	2.02

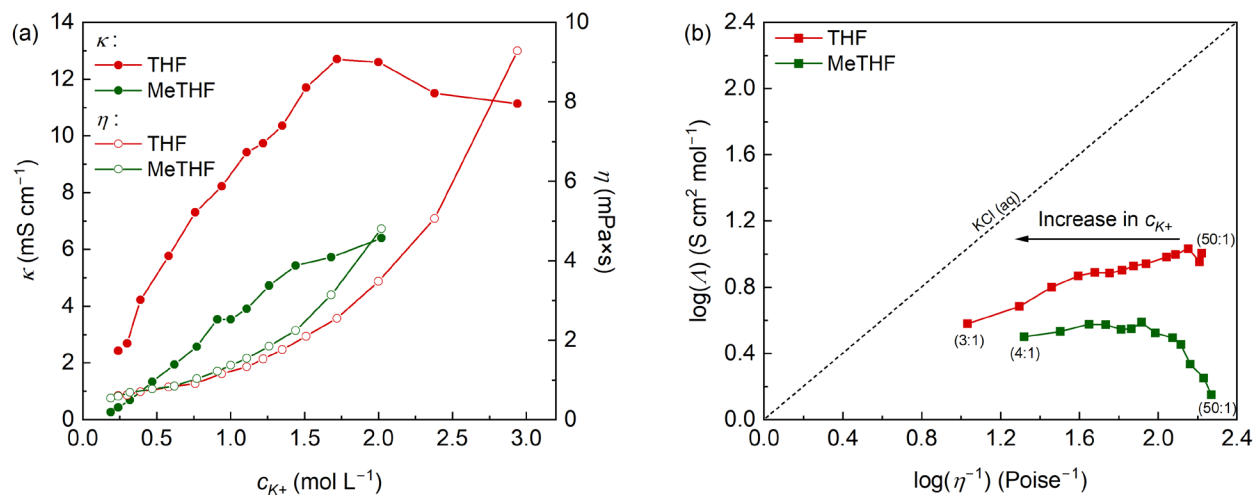


**Figure S1.** (a) Ionic conductivity and dynamic viscosity of the THF/MeTHF-KFSI binary mixtures vs. the  $K^+$  concentration in molarity, measured at 25 °C. (b) Walden plot of the THF/MeTHF-KFSI binary mixtures.

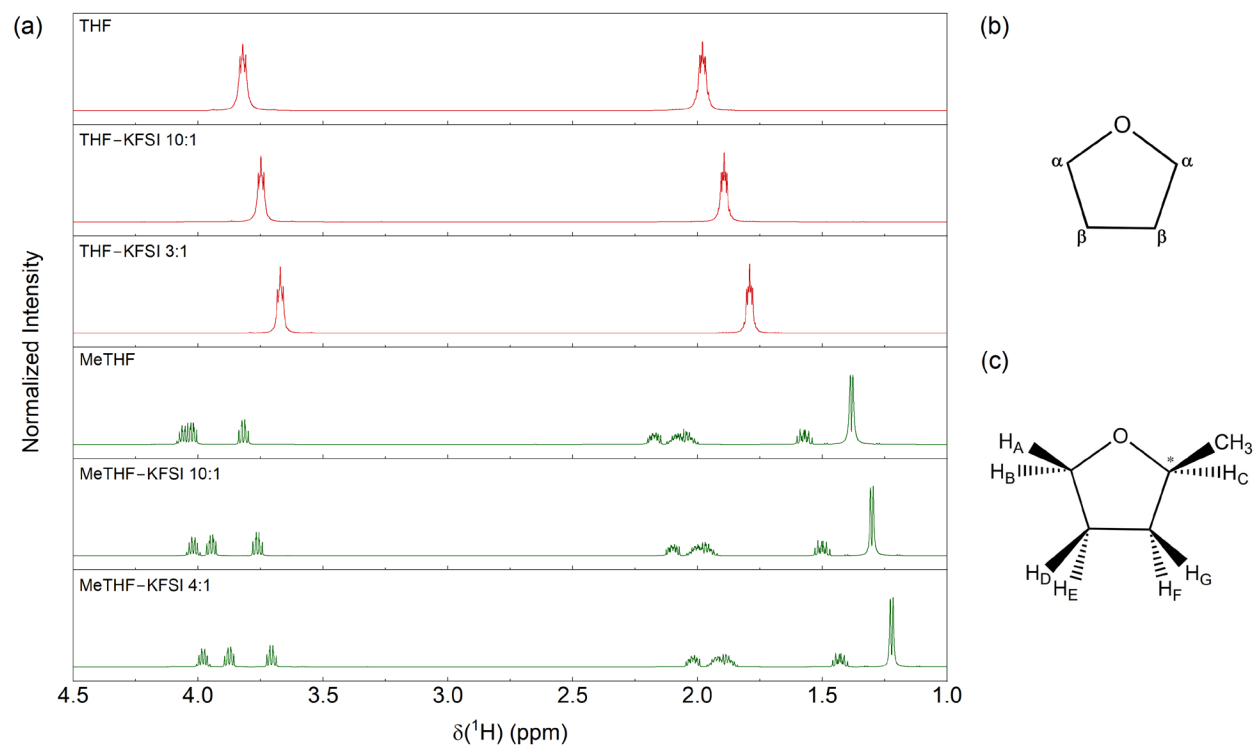


**Figure S2.** (a) Concentration dependence of the  $^1\text{H}$  NMR (600.35 MHz) chemical shifts for THF/MeTHF-KFSI binary mixtures. The spectra were individually, vertically scaled to equal intensity of the largest signal. Structural formula of (b) tetrahydrofuran and (c) (*S*)-2-methyltetrahydrofuran, with the different proton environments assigned.

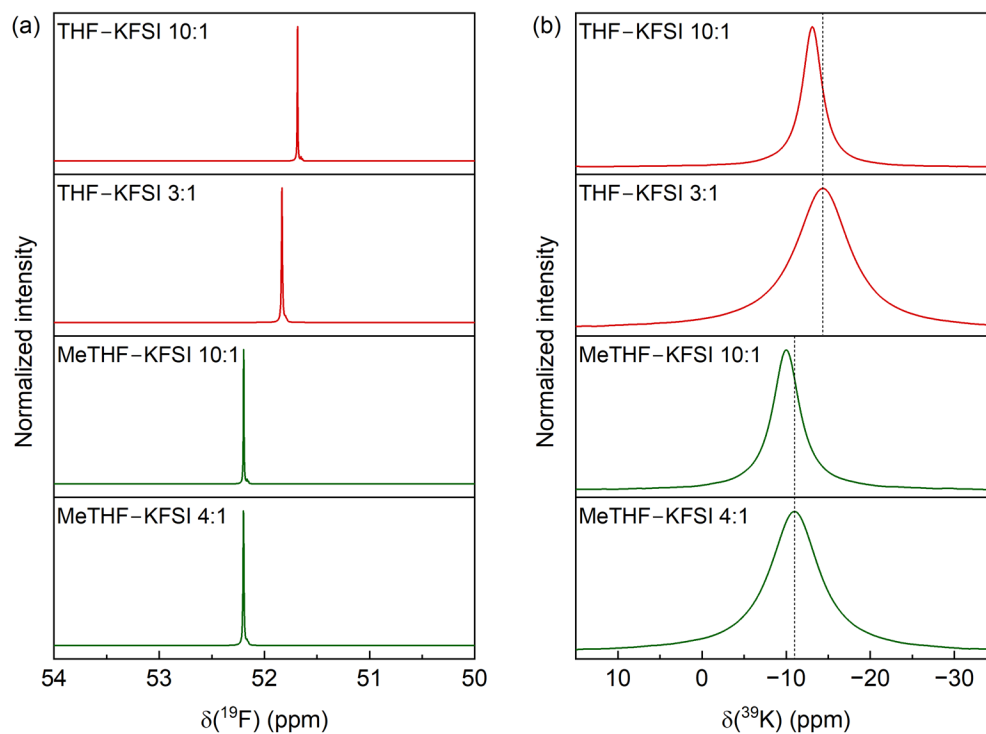


**Figure S3.** Concentration dependence of the  $^{19}\text{F}$  NMR (564.89 MHz, (a)) and  $^{39}\text{K}$  NMR (28.01 MHz, (b)) chemical shifts for THF/MeTHF-KFSI binary mixtures. All spectra were individually, vertically scaled to equal intensity of the largest signal.

**Table S3.** System composition, equilibrated box length, and density for molecular dynamics simulations of the two electrolyte solutions at 298.15 K.

Electrolyte solution	THF / MeTHF	KFSI	Box length $a$ (Å)	$\rho_{\text{calc.}}$ at 298.15 K ( $\text{g cm}^{-3}$ )
THF-KFSI 3:1	750	250	53.13	1.21
MeTHF-KFSI 4:1	800	200	55.42	1.10

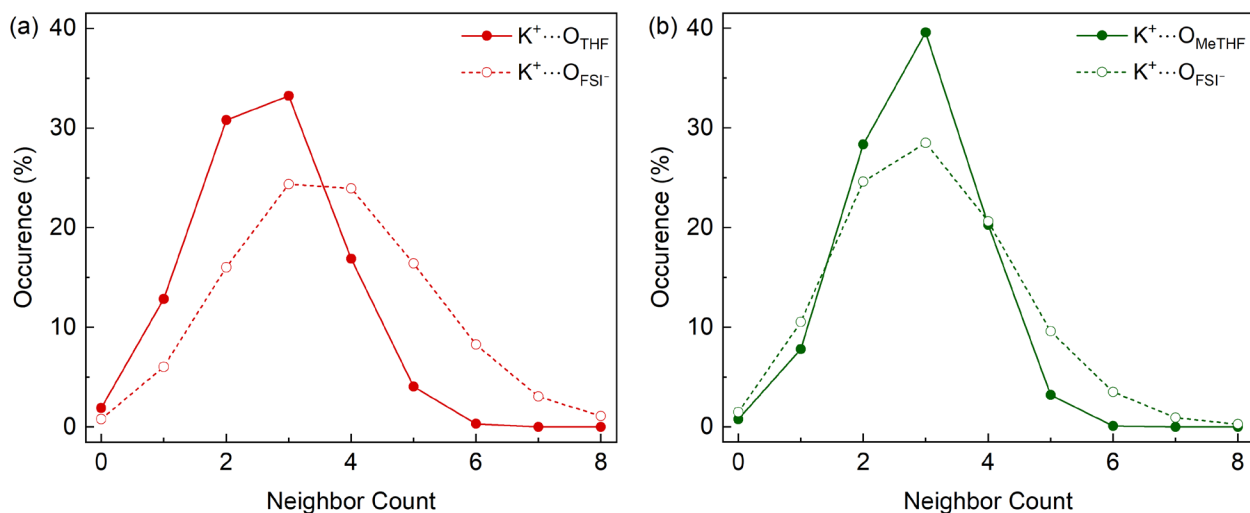


**Figure S4.** Neighbor count histogram for the cation's first solvation shell in (a) THF-KFSI 3:1 and (b) MeTHF-KFSI 4:1.

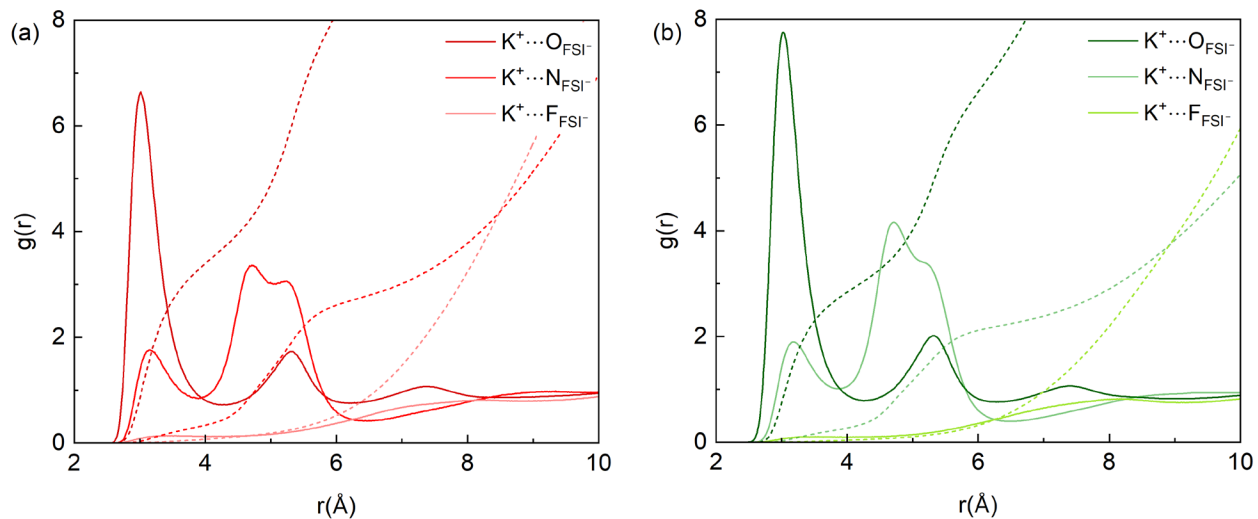


**Figure S5.** Radial distribution functions (solid lines) and number integrals (dashed lines) of the  $K^+$  cation interacting with different atoms of the  $FSI^-$  anion in (a) THF-KFSI 3:1 and (b) MeTHF-KFSI 4:1.

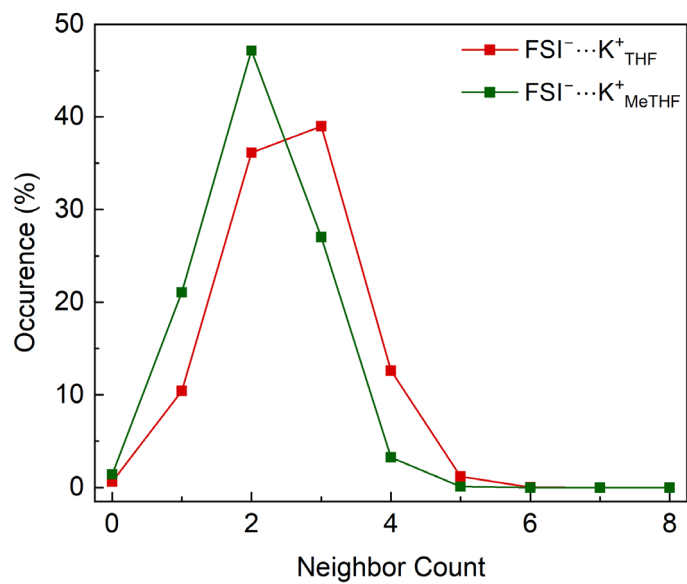


**Figure S6.** Neighbor count histogram for the anion's first solvation shell in THF-KFSI 3:1 and MeTHF-KFSI 4:1.

**Table S4.** Overview of the galvanostatic cycling experiments conducted in K || Al half-cells cycled in THF-KFSI 3:1 and in MeTHF-KFSI 4:1, with two coin cells tested for each cycling condition.

Cell configuration	Electrolyte solution	Coin cell	Cycling conditions	CE <sub>Initial</sub> (%)	Cycle number	$\eta$ First cycle (V)
K    Al	THF-KFSI 3:1	1	0.5 mA cm <sup>-2</sup> 1 mAh cm <sup>-2</sup>	95.4	> 500	0.142
		2		93.6	> 500	0.139
	MeTHF-KFSI 4:1	1		88.7	> 500	0.188
		2		91.6	> 500	0.194
	THF-KFSI 3:1	1	1.0 mA cm <sup>-2</sup> 1 mAh cm <sup>-2</sup>	94.9	> 350	0.196
		2		93.0	> 350	0.192
	MeTHF-KFSI 4:1	1		75.7	> 350	0.274
		2		89.0	> 350	0.249
	THF-KFSI 3:1	1	2.0 mA cm <sup>-2</sup> 1 mAh cm <sup>-2</sup>	93.2	> 200	0.249
		2		97.5	> 200	0.252
	MeTHF-KFSI 4:1	1		74.8	> 150	0.346
		2		82.9	36	0.333
	THF-KFSI 3:1	1	4.0 mA cm <sup>-2</sup> 1 mAh cm <sup>-2</sup>	90.8	104	0.327
		2		98.5	96	0.328
	MeTHF-KFSI 4:1	1		72.5	35	0.422
		2		74.5	29	0.414

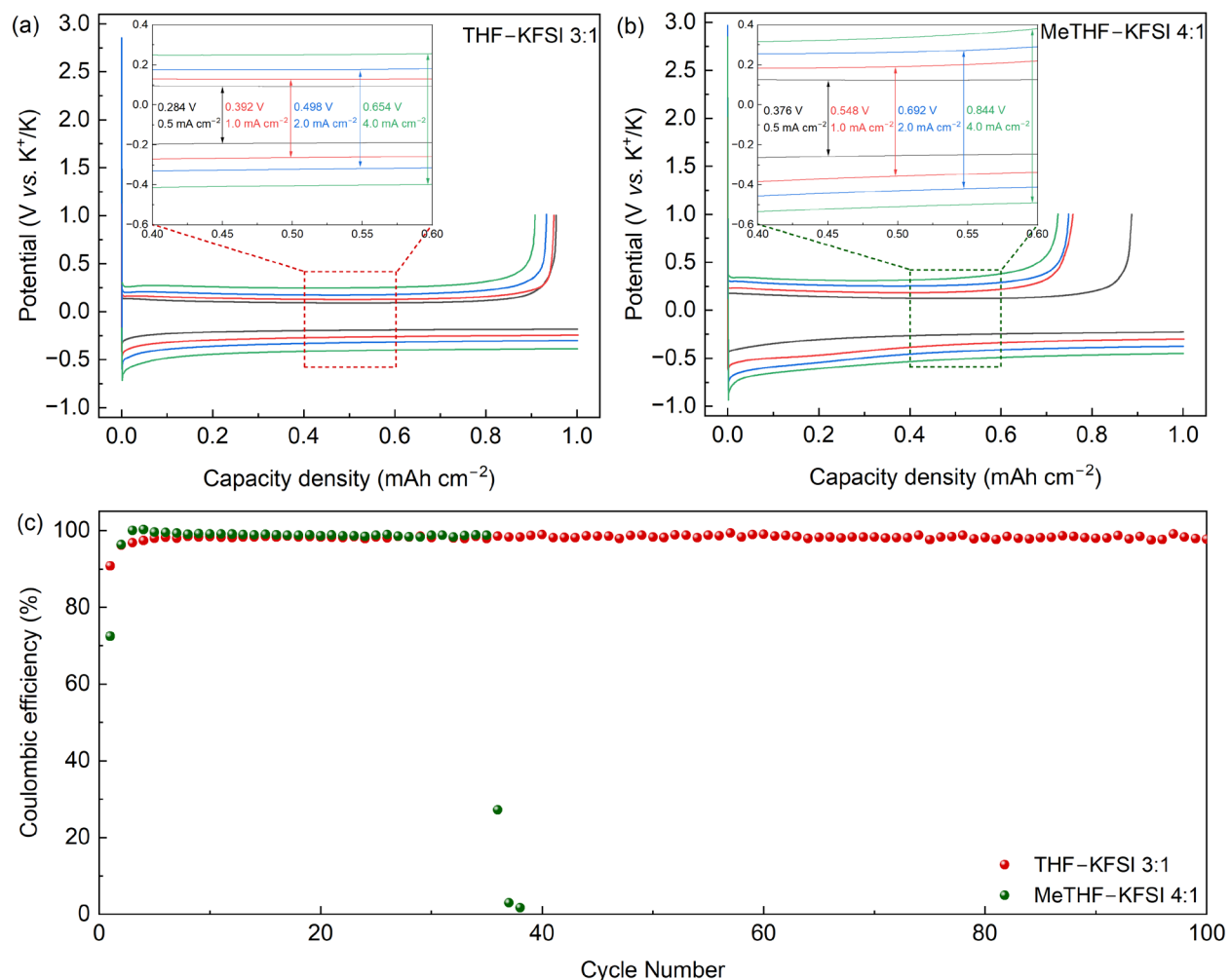


**Figure S7.** Potassium metal plating/stripping behavior in THF/MeTHF-KFSI electrolyte solutions. Polarization profiles of the K||Al half-cell configuration cycled in (a) THF-KFSI 3:1 and in (b) MeTHF-KFSI 4:1 at different current densities with a cutoff capacity of 1 mAh cm<sup>-2</sup>. (c) Potassium metal plating/stripping CE of the K||Al half-cell cycled in different electrolyte solutions at a current density of 4.0 mA cm<sup>-2</sup> with a cutoff capacity of 1 mAh cm<sup>-2</sup>.

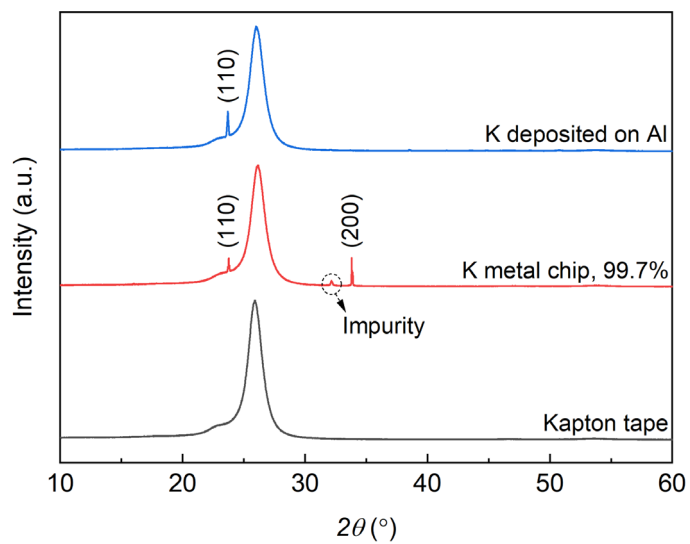


**Figure S8.** X-ray diffraction (XRD) pattern of Kapton tape, potassium metal chip with a purity of 99.7% and potassium metal electrochemically deposited on aluminum foil ( $0.5 \text{ mA cm}^{-2}$ ;  $1 \text{ mAh cm}^{-2}$  – during discharge).

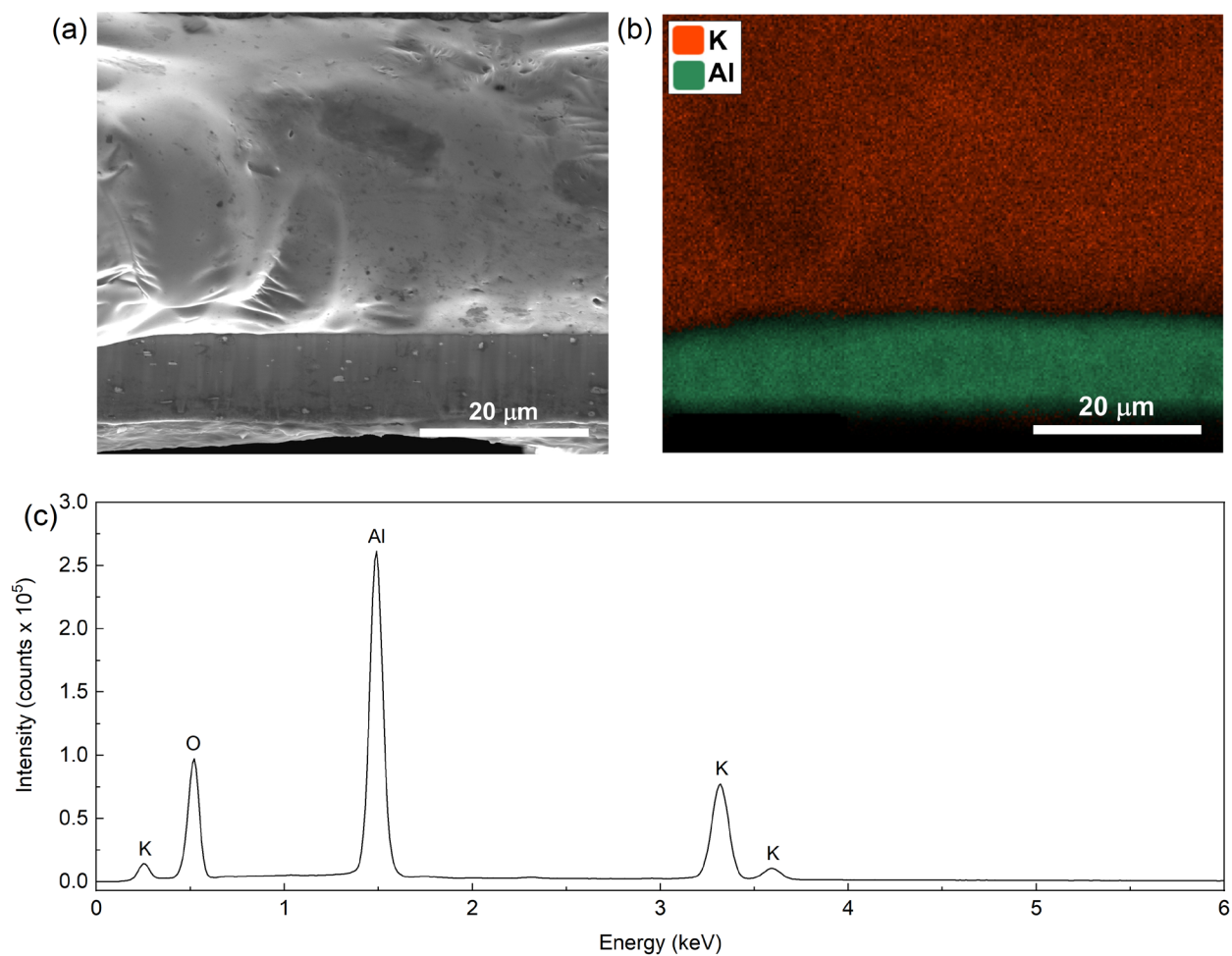


**Figure S9.** (a) SEM cross section image of the deposited potassium metal on the aluminum current collector after discharging of the first cycle at  $0.5 \text{ mA cm}^{-2}$  under  $1 \text{ mAh cm}^{-2}$  in THF-KFSI 3:1. (b) EDX elemental mapping and (c) EDX spectrum of the cross section.

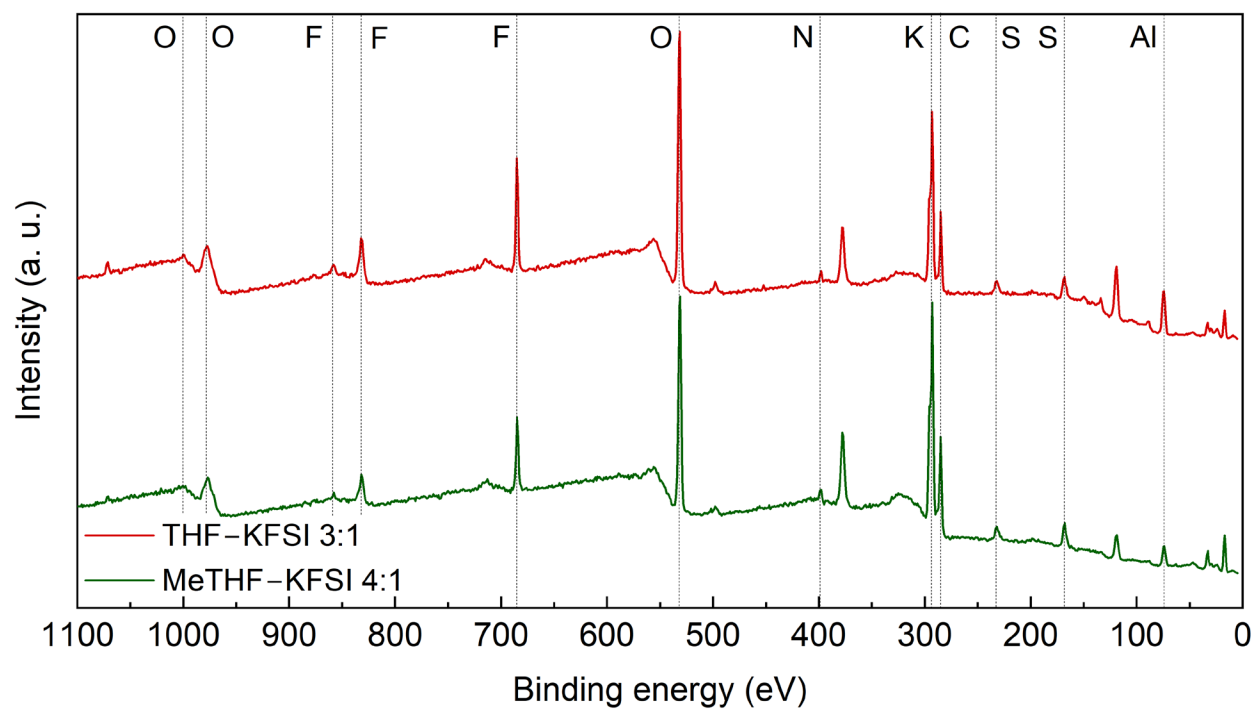


**Figure S10.** XPS profiles of the SEIs formed on the aluminum electrode after the first cycle in THF-KFSI 3:1 and MeTHF-KFSI 4:1.

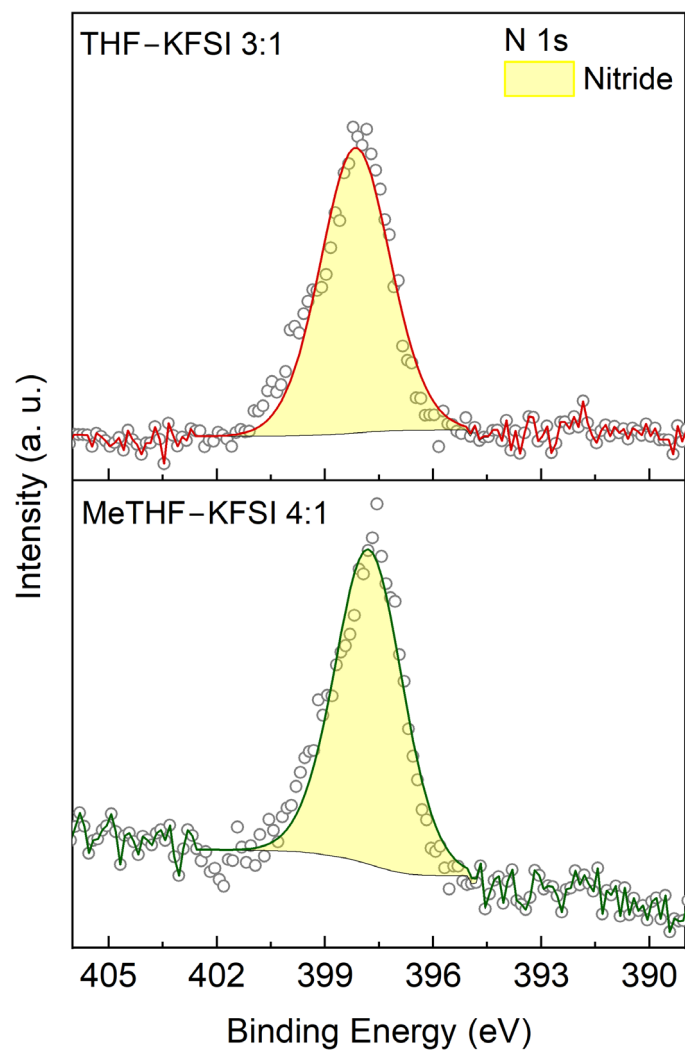


**Figure S11.** N 1s XPS spectra of the SEI layers formed on the aluminum current collector after the first cycle in THF-KFSI 3:1 and MeTHF-KFSI 4:1.

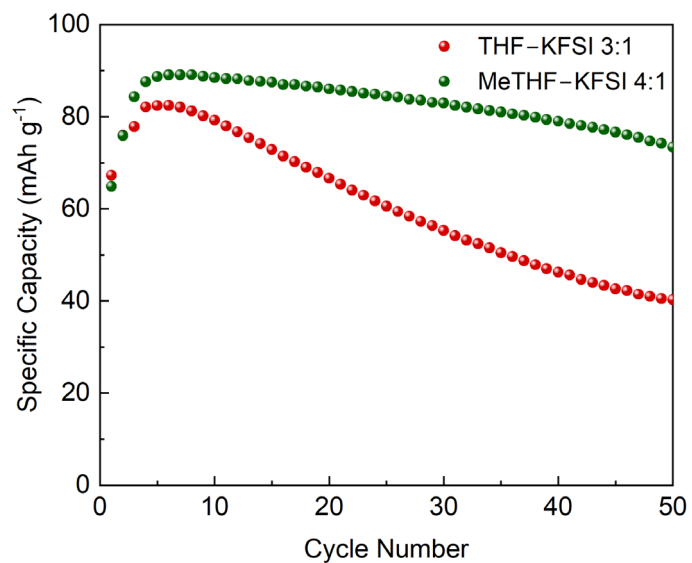


**Figure S12.** Cycling performance of AC | K<sub>2</sub>-Co-PTtSA cells in THF-KFSI 3:1 and MeTHF-KFSI 4:1 at a rate of 0.1C.